Princeton Plasma Physics Laboratory

PPPL- 4917

PPPL- 4917

Towards Identifying The Mechanisms Underlying Field-Aligned Edge-Loss Of HHFW Power On NSTX

Rory Perkins, et. al.

June, 2013

Prepared for the U.S. Department of Energy under Contract DE-AC02-09CH11466.

Princeton Plasma Physics Laboratory
Report Disclaimers

Full Legal Disclaimer

Trademark Disclaimer

PPPL Report Availability

Princeton Plasma Physics Laboratory:

http://www.pppl.gov/techreports.cfm

Office of Scientific and Technical Information (OSTI):

http://www.osti.gov/bridge

Related Links:

U.S. Department of Energy

Office of Scientific and Technical Information

Fusion Links

Towards Identifying The Mechanisms Underlying Field-Aligned Edge-Loss Of HHFW Power On NSTX

R J Perkins[a], J-W Ahn[b], R E Bell[a], A Diallo[a], S Gerhardt[a], T K Gray[b], D L Green[b], E F Jaeger[c], J C Hosea[a], M A Jaworski[a], B P LeBlanc[a], G J Kramer[a], A McLean[b], R Maingi[a], C K Phillips[a], M Podestà[a], L Roquemore[a], P M Ryan[b], S Sabbagh[d], F Scotti[a], G Taylor[a] and J R Wilson[a]

[a]*Princeton Plasma Physics Laboratory, Princeton, NJ*
[b]*Oak Ridge National Laboratory, Oak Ridge, TN*
[c]*XCEL Engineering Inc., Oak Ridge, TN*
[d]*Columbia Univeristy, New York, NY*

Abstract. Fast-wave heating will be a major heating scheme on ITER, as it can heat ions directly and is relatively unaffected by the large machine size unlike neutral beams. However, fast-wave interactions with the plasma edge can lead to deleterious effects such as, in the case of the high-harmonic fast-wave (HHFW) system on NSTX, large losses of fast-wave power in the scrape off layer (SOL) under certain conditions. In such scenarios, a large fraction of the lost HHFW power is deposited on the upper and lower divertors in bright spiral shapes. The responsible mechanism(s) has not yet been identified but may include fast-wave propagation in the scrape off layer, parametric decay instability, and RF currents driven by the antenna reactive fields. Understanding and mitigating these losses is important not only for improving the heating and current-drive on NSTX-Upgrade but also for understanding fast-wave propagation across the SOL in any fast-wave system. This talk summarizes experimental results demonstrating that the flow of lost HHFW power to the divertor regions largely follows the open SOL magnetic field lines. This lost power flux is relatively large close to both the antenna and the last closed flux surface with a reduced level in between, and measurements of the relative amplitude of the inner and outer peaks of heat flux will be discussed. We also address a region of heat deposition on the lower divertor that falls outside the range predicted by field line mapping from the midplane SOL in front of the antenna. To elucidate the role of the onset layer for perpendicular fast-wave propagation with regards to fast-wave propagation in the SOL, a cylindrical cold-plasma model is being developed. This model, in addition to advanced RF codes such as TORIC and AORSA, is aimed at identifying the underlying mechanism(s) behind these SOL losses, to minimize their effects in NSTX-U, and to predict their importance in ITER.

Keywords: ICRF, NSTX, HHFW, RF Heating and Current Drive, Spherical Torus.
PACS: 52.50.Qt, 52.35.-g, 52.55.Fa, 52.70.Gw

INTRODUCTION

Plasma heating using waves in the ion-cyclotron range of frequencies (ICRF) is a primary heating scheme on many fusion devices, including ITER [1], but can be undermined by various loss processes, poor coupling, overheating of antenna components, and injection of impurities. High-harmonic fast-wave (HHFW) heating experiments on the National Spherical Torus eXperiment (NSTX) have identified a significant loss that occurs directly in the SOL as the waves propagate away from the antenna [2,3,4,5,6]. These SOL losses occur prior to the RF power reaching the core plasma since multi-pass damping is essentially negligible on NSTX due to its high beta and consequently high single-pass absorption [2,3,7]. SOL interactions are evident in camera images such as in Fig. 1, where bright streaks emanate from the antenna region and terminate on the upper and lower divertor in bright and hot spirals [4,5]. The flow of HHFW power from the midplane in front of the antenna to the divertor regions is largely along field lines [6] and occurs along all SOL field lines passing in front of the antenna between the antenna and the last closed flux surface (LCFS) and not just those connected to antenna components. The losses are relatively strong along field lines that pass approximately 1 cm inboard of the antenna and also a few millimeters outboard of the LCFS but are relatively weak in between, further indicating that the mechanisms underlying this power loss to the divertor regions are not localized to the antenna components and are distinct from and in addition to the RF sheath losses at the components as described in Refs. [8] and [9]. Such losses can create situations of poor

core heating even with relatively high antenna loading, and such effects must be taken into account in conjunction with any subsequent multi-pass damping that may occur in cases of lower single-pass absorption. For reference, the NSTX HHFW system operates at 30 MHz, contains twelve straps for variable phasing, and possesses a boron-nitride Faraday shield (see Refs. [10] and [11] for details).

The essential questions raised in this paper are 1) whether these field-aligned losses entirely account for the power missing from the core plasma or whether other types of losses are involved, and 2) what are the physical mechanisms responsible for these field-aligned losses? The net effect of all losses is reflected in the amount of RF heating in the core plasma [2,3], and in the case of Fig. 1 (shot 130621, k_φ = -8 m^{-1}, -90° phasing between antenna straps), approximately 40% of the RF power coupled from the antenna reaches the core, meaning that approximately 60% was lost to the SOL (see Fig. 4 in Ref. [4]). Infrared (IR) camera measurements of these spirals show a

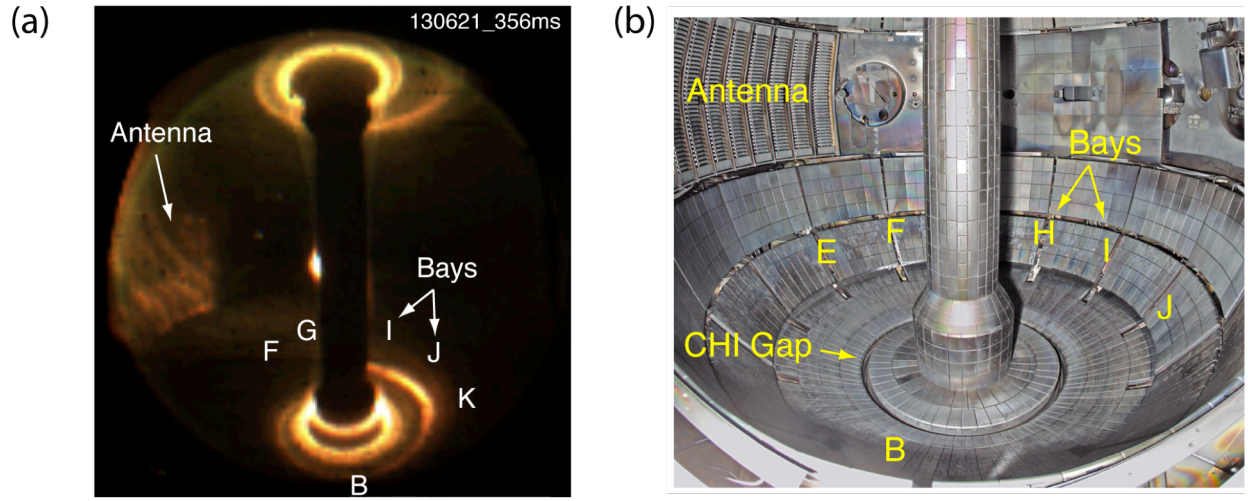

Figure 1. (a) Strong interactions of the HHFW power and the edge plasma are clearly seen in this midplane visible-light image of the spirals on the upper and lower divertor for an ELM-free H-mode plasma with P_{RF} = 1.8 MW. The conditions for shot 130621 are: f_{ANT} = -90°, P_{NB} = 2 MW, I_P = 1 MA, B_T = 0.55 T. b) Vessel image showing position of the antenna, tiles, vessel gap [27], and toroidal bay locations. View rotated 30° toroidally relative to that of (a).

significant RF-produced heat flux to the divertor region, up to ~ 2 MW/m^2 for an RF coupled power of 1.8 MW [5], but the toroidal coverage of the cameras was insufficient to determine quantitatively what fraction of the power missing from the plasma core is accounted for by the total power deposited in the spirals. Other loss mechanism such as associated with parametric decay instability (PDI) [12,13] and with sheath losses on antenna components and adjacent structures connected by magnetic field lines [14,15] undoubtedly make significant contributions as well. As to the underlying cause of the field-aligned losses, the heating efficiency is a strong function of the toroidal wavenumber, k_φ, magnetic field strength, and edge density, suggesting that some of the major loss mechanisms are strongly tied to the location of the onset density for perpendicular fast-wave propagation (righthand cutoff) [2,3,4,5]. We hypothesize that fast waves are propagating in the SOL and dissipating power in the divertor regions either by driving RF sheaths or by setting up streaming RF currents. While measurements of RF fields in the divertor regions will ultimately be needed on NSTX-U to confirm or refute this hypothesis, the possibility can be explored beforehand using state-of-the-art RF codes such as TORIC and AORSA and with simplified cold plasma models.

In this paper, we present a crude estimate of the power dissipated in the spirals that suggests that the field-aligned losses are significant and apparently account for about one half the total power lost. We then summarize experimental observations of the heat spirals, showing that the lost power to the divertor peaks close to both the antenna and also the LCFS, showing that the mechanism underlying the field-aligned SOL losses cannot be localized to field lines emanating from antenna components. On the other hand, field-line mapping suggests that field lines connecting the bottom antenna plate to the lower divertor could explain a region of heat lying outside the mapping from the SOL midplane, suggesting the antenna components are playing some role. Finally, we delve into the possibility of fast-wave propagation in the SOL, outlining a complete cylindrical cold-plasma model. Future modeling and experiments on NSTX-U will of course be required to determine definitively the losses associated with fast-wave propagation in the SOL against the possible contributions from reactive fields/currents excited in front of the antenna, from energetic ions produced by PDI, and from sheath losses to antenna components. The

results presented here are important for verifying RF codes that include the SOL region [16], as these codes must be able to reproduce these edge losses under NSTX conditions so that they can be used for determining the underlying cause(s) and for understanding how to minimize this direct SOL power loss for fast-wave heating, generally.

CRUDE ESTIMATE OF THE POWER LOST WITHIN THE SPIRALS

Presently, the field-aligned losses to the divertor regions appear to account for a significant portion of the HHFW missing in the core plasma, but other losses can also be significant. The limited toroidal coverage of the IR measurements on NSTX and the strong variation of the heat flux along the spiral preclude at present precise quantitative determinations of the total power dissipated within the spirals. However, a very crude estimate of the power deposited can be made by assuming that red spectra emission from the spirals (from the camera view in Fig. 1) is proportional to the amplitude of the RF-produced heat flux to the divertor, Q_{div}. Although the red-pixel intensity is not necessarily proportional to the divertor heat flux, it is observed that, at the end of the RF pulse, the red-pixel intensity decays on a time scale of tens of milliseconds, a timescale expected for heat conduction. An IR camera at Bay I, to be described in the following section, measures the RF-produced heat flux for two sightlines parallel and on either side of the radial vector at Bay I as shown in Fig. 2. The outer deposition peaks of 1.35 MW/m^2 at 34.4^o and 0.7 MW/m^2 at 20^o are noted and exhibit a strong increase in the clockwise direction. For calculating the power deposition over the outer peak, a triangular heat flux deposition profile is assumed (see Fig. 2) with a peak equal to the peak Qdiv and a base equal to the radial width of the SPIRAL-calculated strike points. The wide-angle camera view (Fig. 1) is used to extract the red-pixel intensity along the spiral. Figure 2 plots this red-pixel intensity normalized so that it equals Q_{div} at 34.4^o (Bay I +4.4^o), giving a proxy for Q_{div} along the entire length of the spiral from Bay I to Bay E. This is then used to compute the deposited power, P_{dep}, over 30^o segments of the spiral. P_{dep} over the spiral range in Fig. 2 adds up to 0.335 MW, and with the addition of the other segments of the lower heat spiral and the upper heat spiral, this crude estimate suggests that these field-aligned losses to the divertor regions account for about half of the total RF power loss of approximately 1.1 MW in the case of shot 130621 [4]. Thus, these field-aligned SOL losses to the divertor are very significant and certainly comparable to other losses such as associated with PDI and with sheath losses on antenna. Preparations are underway to greatly increase the toroidal IR coverage on NSTX-U in order to quantify the total power lost in the spirals using measured Q_{div} values.

Determining all relevant SOL damping mechanisms is essential for state-of-the-art RF codes that will be used to predict RF performance in ITER, as such codes are not yet capable of reproducing field-aligned power fluxes in the SOL as observed on NSTX. AORSA runs have shown significant RF fields in the SOL with a strong dependence on

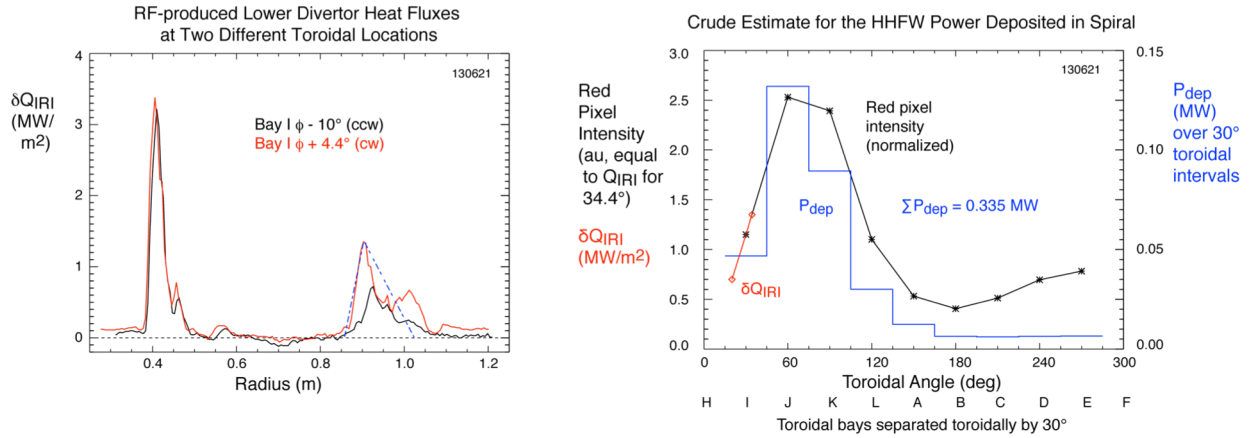

FIGURE 2. (a) δQ_{IRI} vs radius for conditions of Fig. 1 for sightlines parallel to the radius line at Bay I. The angles away from Bay I are given for the peaks of the two curves. Note that CCW is toward Bay H and CW is toward Bay J (see Fig. 1). Data taken at 0.357 s with subtraction from 0.257 s. (b)A crude estimate of the RF power deposited in the spiral can be obtained by using the toroidal variation of the red pixel intensity as a proxy for the variation of the heat flux intensity. The black curve is the red pixel intensity normalized so that two points of the Q_{div} lie on it. The blue curve is then an estimate of the power deposited in each section of the spiral. The total power deposited from Bay I to Bay E is estimated to be around 0.335 MW.

k_φ [16]. However, without the proper damping mechanisms in the edge, the only sink for the RF power is absorption by plasma species, which is inherently weak in the relatively cold edge plasma. Thus, in such simulations, power

cannot be dissipated in the SOL, and the SOL RF field amplitudes build up to the point at which the Poynting flux to the core, where power can be readily absorbed, balances the input power from the antenna. It is thus critical to include the proper physics of SOL wave damping so that such codes can compute the power dissipated and lost in the SOL against the power flowing into the core and from the antenna, and this includes the requirement of accurately measuring the field-aligned losses to the divertor through improved IR coverage.

RADIAL PROFILE OF HHFW LOSSES TO THE DIVERTOR REGION

HHFW power lost in the SOL flows to the divertor region mainly along the magnetic field, as is evidenced by comparing SOL field-line mapping to various measurements of RF-produced effects in the divertor regions [6]. The following section describes the field-line mapping procedure, the IR-camera data processing, and the resulting profile of lost HHFW. The loss profile shows that the associated loss mechanism is not localized to the antenna components but rather extends across the width of the SOL.

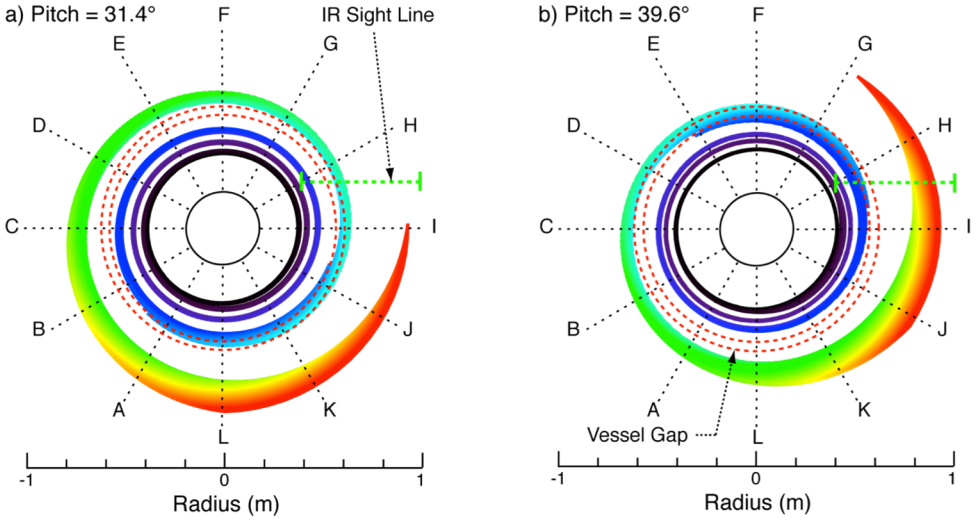

Figure 3. SPIRAL strike points using EFIT02 for the lower divertor floor for different magnetic field pitch (shots 141888 for (a) and 141899 for (b) at t = 0.355 s). As the magnetic pitch increases, the spiral rotates toroidally across the IR sight line. [k_φ = -8m^{-1} (-90°), D_2, P_{RF} = 1.4 MW starting at t = 0.25 s, P_{NB} = 2 MW]

Field-line mapping is done using the SPIRAL code, a full-orbit particle code [17]. The particle orbits produced with SPIRAL can be taken as proxies for the field lines because the particles are launched here with velocities parallel to the magnetic field, which minimizes grad-B drifts, and with low speeds (1 eV deuterons), which minimizes curvature drifts. From a given major radius at the midplane (denoted R_{SOL}), field lines are tracked to the point at which they strike the divertor region, which we refer to as a strike point. Figure 3(a) plots these strike points on the lower divertor floor for a dense set of field lines that includes many different R_{SOL}, from the LCFS to the antenna limiter, as indicated by the color-coding. The set of computed strike points forms a spiral as is observed experimentally (see Fig. 1). In Fig. 3(b), the same procedure is done for a similar plasma with a higher field pitch, resulting in a counter-clockwise rotation of the spiral. The field-line mapping is sensitive to uncertainties in the equilibrium reconstructions, and, while the mappings still generally agree with the data, such uncertainties could be important, for example, in specifying exactly the location of the outer vessel strike radius [18].

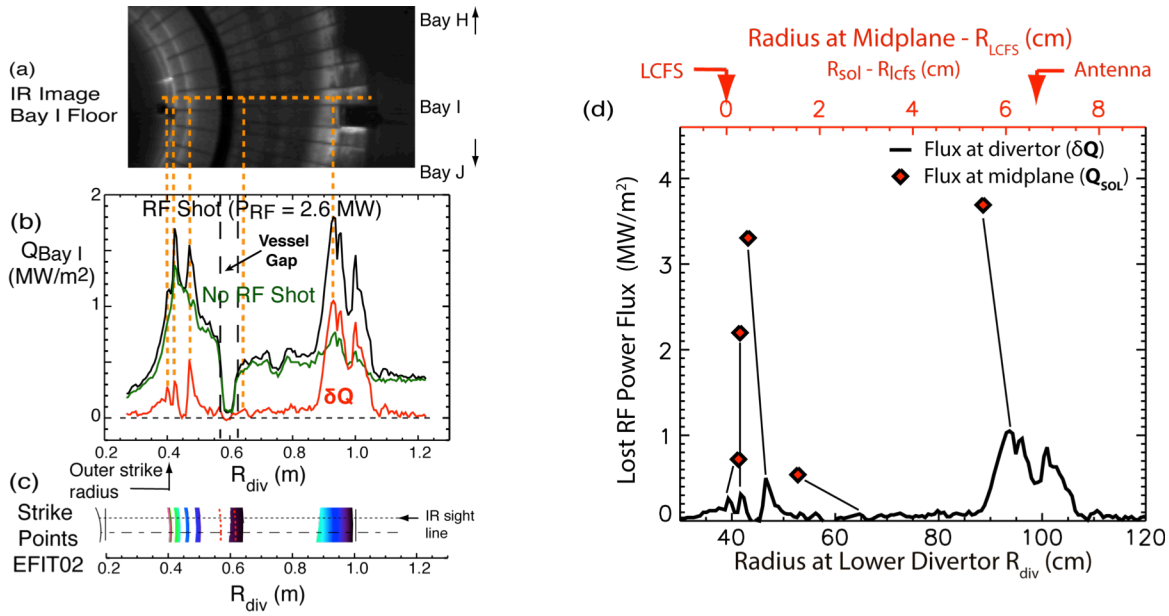

FIGURE 4. RF heat peaks agree with field-line strike points for an ELMy H-mode plasma (shot 135333, no RF shot 135334). (a) Heat-flux image in which multiple passes of the spiral are identifiable. (b) A radial profile of heat flux plotted against divertor radius (R_{div}). (c) Computed strike points at Bay I [ϕ_{ANT} = -90°, P_{NB} = 2 MW, I_P = 0.8 MA, B_{tor} = 0.45 T]. (d) Calculated values of the power lost at the SOL midplane, Q_{sol}, are shown for the peaks of the measured IR profile for the ELMy H-mode plasma (shot 135333). The power lost in the SOL midplane peaks inboard of the antenna and again outboard of the LCFS. (R_{lcfs} = 1.508 m)

The IR camera used in this paper is located at Bay I and is aimed at the lower divertor region. Another camera, aimed at the upper divertor, is available [18], but its measured heated fluxes are relatively weak for the shots analyzed here. The Bay I camera has been calibrated to convert the measured IR emission from a graphite surface into a surface temperature [19]; then, using the THEODORE code [20,21], the time history of the surface temperature is converted into a heat flux normal to the surface. There is an uncertainty of approximately ten to twenty percent in the calibration of the heat-flux data reported here. The heat flux measured with IR cameras contains both the RF-produced heat flux along the SOL field lines and the heat flux ordinarily expelled from the plasma core, whether heated ohmically, through RF waves, or through beams. The total RF-produced heat flux to the divertor can be isolated by subtracting data from a reference shot with identical plasma parameters but no applied RF power. This has been done for an ELMy plasma in Fig. 4; the spiral streaks due to RF heat flux along field lines are clearly seen in Fig. 4(a), and the heat-flux peaks in the lower divertor are clearly resolved even near the outer vessel strike radius in Fig. 4(b). Moreover, the locations of the field-line-mapping strike points at Bay I agree with the location of the heat peaks rather well in Fig. 4(c).

The field-line mapping permits the lower-divertor heat flux peaks to be mapped back to the midplane in front of the antenna. This presumes that the RF power lost to the divertor via the SOL is entirely field-aligned, an assumption that is supported by the above observations (Fig. 4). We compute the z-component (vertical component) of the lost RF power flux at the midplane, Q_{SOL}, from the z-component at the lower divertor, which we denote as Q_{div}. The toroidal component of the field-aligned lost RF heat flux is unimportant for determining the RF power deposited in the divertor regions because it is tangential to the divertor surfaces. There is a flux expansion factor in going from the divertor to the midplane, as the SOL flux surfaces are more spread out at the divertor than at the midplane due to the weakening of the poloidal field. Also, note that only a portion of the lost RF power profile can be obtained at the midplane because the IR camera used here obtains data from Bay I and thus samples only a portion of the HHFW power flow, namely that along field lines whose strike points land in the vicinity of Bay I. Regions of low heat flux shown in Fig. 4(b) do not necessarily correspond to midplane radii with low lost RF-power coupled, as the RF power lost along such field lines lands away from Bay I in the lower divertor region. For this reason, only the local maxima of heat flux, where field lines definitely land at Bay I, are mapped back to the midplane here.

Despite the limited IR-camera coverage, an indication of the lost radial power profile across the SOL midplane is still obtained, as shown in Fig. 4(d) for the ELMy case. The lower curve is the δQ obtained above plotted as a function of major radius at the lower divertor in the vicinity of Bay I. Each peak of these curves is mapped back to the midplane, represented by the upper horizontal axis that is the midplane major radius (R_{SOL}) minus the radius of the LCFS (R_{LCFS}). The lost power is relatively large both close to the antenna and also again near the LCFS, peaking a few centimeters inboard of the antenna and a few millimeters outboard of the LCFS. Multiple IR cameras or a single wide-angle lens camera are required to obtain a more complete recovery of the radial loss profile in the SOL. The observed drop between the antenna and LCFS is consistent with the weak power deposition of the second spiral pass at Bay I and is discussed more fully in Ref. [22].

THE ROLE OF FIELD LINES CONNECTED TO THE BOTTOM ANTENNA PLATE

The results of the previous section show that the mechanism behind the field-aligned losses to the divertor cannot be localized to field lines connected to antenna components. However, field lines connecting the inboard edge of the bottom plate of the antenna to the lower divertor appear to be responsible for the outermost heat deposition measured by the Bay I IR camera for the magnetic pitch scan analyzed in Ref. [6]. Figure 5(a) compares the IR data to the computed strike points along a sight line near Bay I (see Fig. 3) for each shot in the pitch scan; both the first and second peaks of the spirals are apparent for all shots except 141888, for which only the "second" pass peak is visible at Bay I. IR data were not obtained at smaller radii due to technical difficulties with the camera. Beneath each IR plot are the computed strike points; the colored points comes from field lines connected to the midplane in front of the antenna, while the black points connect to the bottom plate of the antenna, as will be described below. The locations of the IR peaks are in good agreement with the field lines connected to the midplane in front of the antenna (colored points), but a non-trivial patch of heat that lands outboard of these points. Importantly, the second

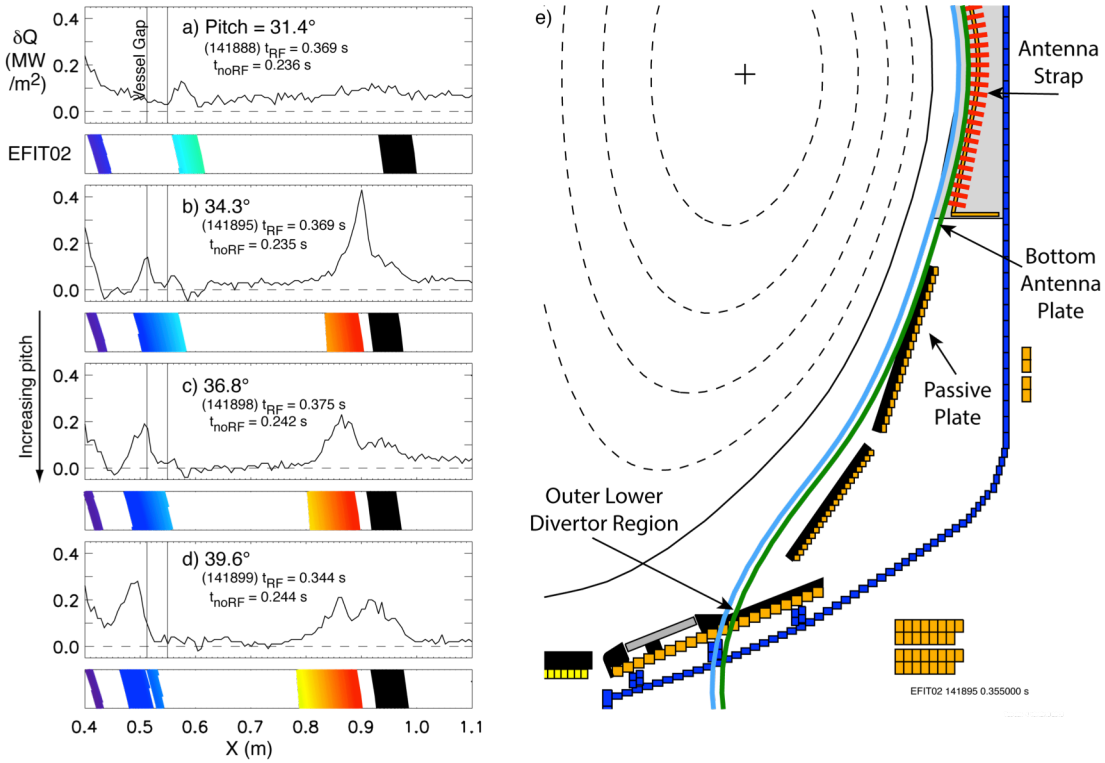

FIGURE 6. (a-d) IR data from Bay I plotted against X, the distance along the sight line, and SPIRAL strike points from the midplane (colored) and from the edge of the bottom antenna plate (black) for shots in a pitch scan. The IR data are taken at the times shown, and EFIT02 equilibrium fits are taken at 355 ms. (e) Light blue line indicates the field line touching the antenna limiter at the midplane. The green line grazes the side passive plate. The space between the curves contains the field lines connecting the lower divertor to the inboard edge of the bottom antenna plate and apparently explains the observed outer heat flux.

pass of the spiral moves inward radially with increasing magnetic pitch, as did the first pass in Ref. [6], and the strike points track this motion over the gap in the vessel floor. For the low pitch case of shot 141888, the computed strike points do not reach Bay I on the first pass as indicated by the absence of strike points at large radii (see Fig. 3 as well), and there is correspondingly no RF-produced heat-flux peak in the IR data.

For shots 141895, 141898, and 141899, there is a substantial additional heat flux outboard of the colored SPIRAL strike points, which connect to the midplane in front of the antenna. This outer heating is not due to a deviation of the HHFW power flow from field lines because the field-line mapping agrees quite well with the position of the second heat peak, which has a greater connection length to the midplane. Instead, this additional RF-produced heat flux at such large radii can be attributed to power flow along field lines connected to the edge of the antenna bottom plate. The colored strike points shown in Fig. 5(a-d) and in previous publications included field lines that, at the midplane, reach out to R = 1.575 m, which is the major radius of the antenna limiter at the midplane. However, as shown in the poloidal cross-section in Fig. 5(e), there are field lines even further out that miss the side passive plate and connect to the edge of the bottom antenna plate to the outer divertor region. The outer radial limit of such field lines is set by the passive side plate. The black strike points in Fig. 5(a-d) are produced by SPIRAL calculations for such fields lines, and they extend the strike point pattern over the region of outer heating in Fig. 5(a-d). It has been observed that field lines connected to antenna components can have enhanced plasma potential due to RF electric fields normal to the surface so that large sheath potentials and power dissipation can occur at the other end of the field line, in this case the lower divertor [Refs needed]. It is also possible that propagating-wave effects can extend to the wall and antenna bottom plate. The location of the black strike points depends on the magnetic pitch as for the SOL midplane lines. For the relatively low pitch of shot 141888, the black strike points in Fig. 5(a) connect to near the counter-clockwise bottom corner of the antenna box for which the potential can be expected to decrease relative to the center of the bottom plate. Thus, a relatively small value of approximately 0.1 MW/m^2 of RF-produced heat flux is just discernable at large radii for shot 141888 (Fig. 5(a)).

ON THE POSSIBILITY OF FAST-WAVE PROPAGATION IN THE SOL

Fast-wave propagation in the SOL has been proposed as the mechanism behind the field-aligned HHFW power losses to the divertor with power dissipation occurring on the divertor due to RF-sheath rectification (far-field effect) or by RF currents generating non-linear plasma heating. This hypothesis is motivated by the strong correlation of heating efficiency with the location of the onset density for perpendicular fast-wave propagation. Below this density, the perpendicular wavenumber is imaginary, and if the antenna is too far from the plasma the wave fields evanesce substantially before reaching the core plasma, resulting in poor antenna loading. However, on NSTX, moving this cutoff density too close to the antenna significantly lowered heating efficiencies, perhaps by promoting significant fast wave propagation in the SOL. Further evidence for this hypothesis is that the field-aligned losses are not localized to the antenna but rather occur across the SOL, rising to relatively large amplitudes near the LCFS as indicated by Fig 4(d). This radial profile of lost HHFW power could be indicative of a radial standing-wave pattern in a cavity due to partial reflections of the waves off the steep pedestal gradient.

To explore the possibility of fast-wave propagation in the SOL, a cylindrical cold-plasma model is being developed that includes a high-density cylinder of plasma surrounded by a lower-density annulus to model the SOL. The model is a complete cold plasma theory in that it retains the mass of the electron and thus keeps both roots of the dispersion relation. Though the geometry is greatly simplified and hot plasma and non-linear effects are not included, the model will determine the amount of wave power propagating in the annulus (SOL) against that in the core by varying the density of the annulus above and below the onset density for perpendicular propagation. The model will also test for how closely the Poynting flux follows the fields lines. The model will guide future experimental work and also work with larger and more complicated RF codes that are also under development to address the SOL issues discussed above.

CONCLUSIONS

Experiments on NSTX have exhibited significant field-aligned losses of HHFW power that are subsequently deposited on the upper and lower divertor. These losses are not localized to field lines connected to the antenna; power is lost strongly along field lines close to the antenna and close to the LCFS but not in between. While an accurate measurement of the total power deposited in the spirals is not yet available, a crude estimate based on the toroidal dependence of red-pixel light suggests that these field-aligned losses to the divertor account for a significant

portion (up to half) of the coupled HHFW power that is lost outside the core plasma. Other loss mechanisms including sheath losses to antenna components and magnetically connected structures and PDI-produced losses may play a comparable role. Indeed, losses along field lines connecting the bottom antenna plate to the lower divertor are significant. The critical questions to be addressed on NSTX-U are how and where the HHFW power is converted into a heat flux. It appears that the underlying mechanism is related to fast-wave propagation in the SOL [7,8] possibly resulting in RF-driven sheaths at the plates, ohmic losses in divertor tiles due to RF return currents, and/or direct RF non-linear plasma heating along the field lines leading to the divertor plate. Direct measurements of RF fields will be utilized on NSTX-U to verify fast-wave propagation in the SOL and to explore sheath and RF-current losses at the divertor plates, but before then modeling efforts, ranging from complete cold-plasma theory to codes such as TORIC and AORSA, will explore the possibility of significant fast-wave propagation in the SOL and how that depends on the location of the onset density layer. Indeed, these field-aligned losses obtained on NSTX provide a clear test for verifying RF codes that treat the SOL region and damping processes there.

The field-aligned RF losses studied here could impact other fusion devices, including ITER. While the losses to the divertor region along field lines have been studied here on NSTX, a spherical torus with relatively high magnetic pitch, field-aligned ICRF-effects in the SOL, such as erosion and impurity production [23,24,25], have also been observed under conventional-tokamak conditions and indicate these effects are common to fast-wave systems. The strength of these field-aligned effects are sensitive to the edge density, magnetic field strength, and antenna wavenumber, which vary from machine to machine. These losses to the divertor may also be more apparent on NSTX because the increased field pitch causes the spiral to be less 'sheared' than in a conventional tokamak, and a low-shear spiral is more readily observed. Moreover, other loss mechanisms are in action as well. Again, in order to reliably predict the ICRF performance on ITER, state-of-the-art RF codes must be validated by including the proper SOL wave-damping physics to reproduce these losses under NSTX-like conditions.

ACKNOWLEDGMENTS

This work is supported by USDOE Contract No. DE-AC02-09CH11466.

REFERENCES

[1] D. W. Swain and R. H. Goulding, *Fusion Eng. Des.*, vol. 82, p. 603, 2007.
[2] J. C. Hosea et al., *Phys. Plasmas*, vol. 15, p. 056104, 2008.
[3] C. K. Phillips et al., *Nucl. Fusion*, vol. 49, p. 075015, 2009.
[4] J. C. Hosea et al., *AIP Conf. Proc.*, vol. 1187, p. 105, 2009.
[5] G. Taylor et al., *Phys. Plasmas*, vol. 17, p. 056114, 2010.
[6] R. J. Perkins et al., *Phys. Rev. Lett.*, vol. 109, p. 045001, 2012.
[7] M. Ono et al., *Phys. Plasmas*, vol. 2, p. 4075, 1995.
[8] P. Jacquet et al., *Nucl. Fusion*, vol. 51, p. 103018, 2011.
[9] D. A. D'Ippolito et al., *Nucl. Fusion*, vol. 38, p. 1534, 1988.
[10] P. M. Ryan et al., *Fusion Eng. Des.*, vol. 56-57, p. 569, 2001.
[11] P. M. Ryan et al., *AIP Conf. Proc.*, vol. 1406, p. 101, 2011.
[12] J. R. Wilson et al., *AIP Conf. Proc.*, vol. 787, p. 66, 2005.
[13] T. M. Biewer et al., *Phys. Plasmas*, vol. 12, p. 056108, 2005.
[14] L. Colas et al., *J. Nucl. Mater.*, vol. 363-365, p. 555, 2007.
[15] Vl. V Bobkov et al., *Nucl. Fusion*, vol. 50, p. 035004, 2010.
[16] D. L. Green et al., *Phys. Rev. Lett.*, vol. 107, p. 145001, 2011.
[17] G. J. Kramer et al., *Plasma Phys. Contr. F.*, vol. 55, p. 025013, 2013.
[18] J. C. Hosea et al., in *these proceedings*.
[19] D. Mastrovito et al., *Rev. Sci. Instrum.*, vol. 74, p. 5090, 2003.
[20] A. Hermann et al., in *28th EPS Conference on Plasma Physics*, vol. 25, 2001, p. 2109.

[21] A. Herrmann et al., *Plasma Phys. Contr. F.*, vol. 37, p. 17, 1995.
[22] R. J. Perkins et al., *Nucl. Fusion*, submitted.
[23] J-M Noterdaeme et al., *Fusion Eng. Des.*, vol. 12, p. 127, 1990.
[24] S. Wukitch et al., *AIP Conf. Proc.*, vol. 933, p. 75, 2007.
[25] S. Wukitch et al., *J. Nucl. Mater.*, vol. 363-365, p. 491, 2007.

The Princeton Plasma Physics Laboratory is operated
by Princeton University under contract
with the U.S. Department of Energy.

Information Services
Princeton Plasma Physics Laboratory
P.O. Box 451
Princeton, NJ 08543

Phone: 609-243-2245
Fax: 609-243-2751
e-mail: pppl_info@pppl.gov
Internet Address: http://www.pppl.gov